

This item is the archived peer-reviewed author-version of:

Microbial food from light, carbon dioxide and hydrogen gas : kinetic, stoichiometric and nutritional potential of three purple bacteria

Reference:

Spanoghe Janne, Vermeir Pieter, Vlaeminck Siegfried.- Microbial food from light, carbon dioxide and hydrogen gas : kinetic, stoichiometric and nutritional potential of three purple bacteria
Bioresource technology - ISSN 1873-2976 - 337(2021), 125364
Full text (Publisher's DOI): <https://doi.org/10.1016/J.BIORTECH.2021.125364>
To cite this reference: <https://hdl.handle.net/10067/1787520151162165141>

1 **MICROBIAL FOOD FROM LIGHT, CARBON DIOXIDE AND HYDROGEN GAS:**
2 **KINETIC, STOICHIOMETRIC AND NUTRITIONAL POTENTIAL OF THREE**
3 **PURPLE BACTERIA**

4 Janne Spanoghe^a, Pieter Vermeir^b, Siegfried E. Vlaeminck^{a*}

5 ^aResearch Group of Sustainable Energy, Air and Water Technology (DuEL), Department of Bioscience
6 Engineering, University of Antwerp, Groenenborgerlaan 171, 2020 Antwerpen, Belgium

7 ^bLaboratory for Chemical Analysis, Department of Green Chemistry and Technology, Ghent University,
8 Valentin Vaerwyckweg 1, 9000 Gent, Belgium

9 *For correspondence. E-mail siegfried.vlaeminck@uantwerpen.be

10 **ABSTRACT**

11 The urgency for a protein transition towards more sustainable solutions is one of the
12 major societal challenges. Microbial protein is one of the alternative routes, in which
13 land- and fossil-free production should be targeted. The photohydrogenotrophic growth
14 of purple bacteria, which builds on the H₂- and CO₂-economy, is unexplored for its
15 microbial protein potential. The three tested species (*Rhodobacter capsulatus*,
16 *Rhodobacter sphaeroides* and *Rhodopseudomonas palustris*) obtained promising growth
17 rates (2.3-2.7 d⁻¹ at 28°C) and protein productivities (0.09-0.12 g protein L⁻¹ d⁻¹),
18 rendering them likely faster and more productive than microalgae. The achieved protein
19 yields (2.6-2.9 g protein g⁻¹ H₂) transcended the ones of aerobic hydrogen oxidizing
20 bacteria. Furthermore, all species provided full dietary protein matches for humans and
21 their fatty acid content was dominated by vaccenic acid (82-86%). Given its kinetic and
22 nutritional performance we recommend to consider *Rhodobacter capsulatus* as a high-
23 potential sustainable source of microbial food.

24

25 **Keywords:** Single-cell protein; Hydrogen economy; Purple non-sulphur bacteria;
26 Photoautotrophy; Essential amino acids

27 **1 INTRODUCTION**

28 The sustainable production of food and feed is one of the major societal challenges of
29 the 21st century. Firstly, the current production chain is severely altering
30 biogeochemical cycles of nitrogen and phosphorus, biodiversity and land-use, with
31 flows towards the biosphere and oceans that are exceeding the planetary boundaries
32 (Campbell *et al.* 2017). Secondly, it is estimated that by 2050, there will be a 50%
33 higher protein demand, with increases up to 82 and 102% for dairy and meat products
34 respectively (Boland *et al.* 2013). This illustrates the urgency for a protein transition
35 towards more sustainable solutions to secure the global feed and food supply.

36
37 Relevant alternatives are plant-, insect-, and microorganism-based protein products.
38 Microorganisms have among the highest protein content of all organisms, and the use of
39 biomass (e.g. bacteria, algae, yeast and other fungi) for feed or food purposes has been
40 coined ‘single cell protein’ or ‘microbial protein’ (MP). Traditionally, the production of
41 MP was predominantly focused on the use of agricultural products or fossil fuels (land-
42 and fossil-based) as electron donors and/or carbon sources (Alloul *et al.* 2021).
43 Pikaar *et al.* (2018) showed that MP produced on sugar cane waste (land- and fossil-
44 based) could lower global crop area use, global nitrogen losses from croplands and
45 agricultural greenhouse gas emissions by respectively 10%, 2% and 1%. However,
46 land- and fossil-free MP production on renewably produced hydrogen gas could lower
47 the pressure even more by 12%, 7% and 9% respectively. This indicated the need to
48 uncouple from agriculture or non-renewable fossil fuels for MP production.

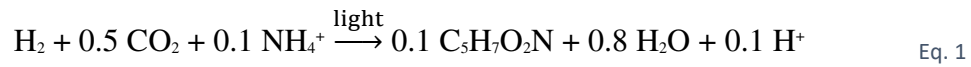
49 Current routes that are being targeted for land- and fossil-free MP production are
50 (phototrophic) microalgae, aerobic hydrogen oxidizing bacteria, methylotrophs or
51 acetotrophs (Alloul *et al.* 2021). Other appealing microbes for MP production are the
52 purple bacteria (PB). The photoheterotrophic PB have been extensively studied on both
53 production routes, with a focus on wastewater streams, and nutritional quality (Capson-
54 Tojo *et al.* 2020). However, literature on the photoautotrophic growth of PB, all purple
55 non-sulphur bacteria (PNSB), with H₂-gas as electron donor (hydrogenotrophic) is
56 limited and lacks nutritional characterization (Douthit and Pfennig 1976, Madigan and
57 Gest 1979, Colbeau *et al.* 1980, Wang *et al.* 1993, Rey *et al.* 2006). Nevertheless, this
58 metabolism is of high interest as it can be applied on sustainable and renewable
59 resources for energy, electron donor and C/N/P/..., while decoupling from arable land
60 by using:

- 61 1. Light energy from the sun or generated via renewable energy
- 62 2. Electrons from H₂, from water electrolysis based on renewable energy, syngas
63 from organic waste streams, or from biohydrogen produced by PB
64 photofermentation of organic waste streams (Capson-Tojo *et al.* 2020)
- 65 3. Sequestered carbon (carbon capture and utilization), for instance from flue gas
66 or other CO₂-rich exhaust gases
- 67 4. Nutrients (N and P), sourced from sustainable production or recovery from
68 waste streams (e.g. (NH₄)₂SO₄ and struvite)"

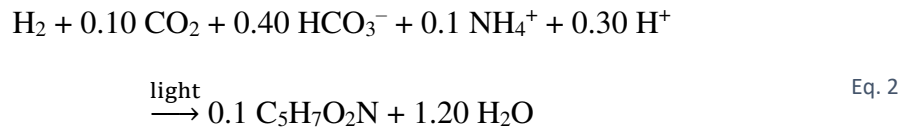
69

70 A stoichiometric equation for photohydrogenotrophic PB growth can be derived by
71 balancing electrons, charges and elements (C, H, N and O) assuming (i)

72 photolithoautotrophic growth reducing inorganic carbon with H₂, (ii) ammonium as
73 nitrogen source, (iii) a generic microbial biomass formula (C₅H₇O₂N):



74 Using the expected inorganic carbon equilibrium at pH 7 (28°C) yields:



75 In order to compare the performance of these photohydrogenotrophic PB, microbial
76 protein sources with metabolic similarities are used as a reference point. These are
77 photoautotrophic microalgae, photoheterotrophic PB and hydrogenotrophic hydrogen
78 oxidizing bacteria (HOB).

79

80 It is hypothesized that the metabolic versatility of PB can yield a high tunability of the
81 essential amino acids (EAA), and in extension their nutritional quality, rendering them
82 one of the most attractive MP types (Alloul *et al.* 2021). This tunability was previously
83 seen for photoautotrophic microalgae by species selection or cultivation-based
84 optimization (e.g. nitrogen levels, light intensity and growth phase) (Sui and Vlaeminck
85 2018, Muys *et al.* 2019, Sui *et al.* 2019). Besides the production of protein, PB contain
86 an array of by-products that enrich the nutritional quality further, such as fatty acids,
87 carotenoids, phytohormones and vitamins and promising results were seen already in
88 feeding trials (Capson-Tojo *et al.* 2020).

89

90 In this study, the kinetic and nutritional properties of the photohydrogenotrophic growth
91 for three PNSB were described (*Rhodobacter capsulatus*, *Rhodobacter sphaeroides* and
92 *Rhodospseudomonas palustris*). The maximum growth rates, biomass productivities,

93 yields, protein productivities, protein quality (EAA profile), fatty acids and pigment
94 content will be examined through batch cultivation at 28°C. To our knowledge, this
95 paper will be the first determination of all these aspects. Previous literature only briefly
96 discussed maximum growth rates, often only as a subsection of a study. Furthermore,
97 the first verification of dietary protein match for different target organisms (humans,
98 pigs and penaeidae shrimp) will be made, giving insight into the nutritional tunability
99 among the 3 PB species. This study will broaden the knowledge of land- and fossil-free
100 production of PB, providing the foundation for the utilization to its full potential as MP
101 for feed and food.

102 **2 MATERIAL AND METHODS**

103 **2.1 SPECIES**

104 Three species were tested in this study of which *Rhodobacter capsulatus* (*Rh.*
105 *capsulatus*) was obtained from Alloul *et al.* (2019) whom isolated it from a mixture of
106 activated sludge from a sewage treatment plant, activated sludge from a dairy
107 wastewater treatment plant and sediment from a local pond, after which it was identified
108 by high-throughput 16S rRNA sequencing (Illumina MiSeq; V4 region). *Rhodobacter*
109 *sphaeroides* (*Rh. sphaeroides*) (strain: LMG 2827) and *Rhodopseudomonas palustris*
110 (*Rps. palustris*) (strain: LMG 18881) were ordered from BCCM (Belgian Coordinated
111 Collections of Microorganisms). Originally, all these species were
112 photoheterotrophically enriched from their environments. The three species were stored
113 in aliquots at -80°C and new series of experiments were always started with a fresh
114 aliquot to keep cultures pure, and experiments reproducible.

115 **2.2 GROWTH MEDIUM**

116 The growth medium used was based on Madigan and Gest (1979), yet adapted in the
117 dosage of carbon, nitrogen and phosphorus. Inorganic carbon was dosed as NaHCO_3
118 instead of CO_2 in the gas phase in a concentration of 0.33 g-C L^{-1} (27 mM), while
119 nitrogen was dosed as $(\text{NH}_4)_2\text{SO}_4$ in a concentration of 0.31 g-N L^{-1} (22 mM). To
120 counteract the consumption of H^+ during photohydrogenotrophic growth, a phosphate
121 buffer system was used. The buffer strength in the medium of Madigan and Gest (1979)
122 was 20 mM, which yielded a fast and high increase in pH that went above pH 8. This
123 had to be avoided to prevent the formation of CO_3^{2-} in the medium. Also, other tested
124 buffers (HEPES and tris) did not control the pH sufficiently within these limits in
125 strengths varying from 10-30 mM. As a result, the monobasic potassium phosphate
126 (KH_2PO_4) was dosed in a concentration of 0.93 g-P L^{-1} (30 mM) which controlled the
127 pH below 8. Nitrogen and phosphorus were thus supplied in excess.

128 **2.3 BATCH GROWTH TESTS**

129 Batch growth tests were performed with Erlenmeyer flasks of 500 mL (DURAN,
130 Germany), with a working volume of 300 mL. At first the autoclavable components of
131 the growth medium were added, after which the bottles were autoclaved at 121°C for 25
132 minutes. Then the remaining medium components were axenically added after filter
133 sterilization ($0.20 \mu\text{m}$), while inoculum was added last. The initial biomass
134 concentration was set at an optical density of 0.05 at 660 nm. The Erlenmeyer's were
135 subsequently closed with a gas-tight septum (DURAN, Germany) and the headspace
136 was flushed for 1 minute with a mixture of 80% H_2 /20% N_2 at a rate of 1.25 L min^{-1} and
137 set at a gauge pressure of +0.4 bar (absolute pressure 1.4 bar).

138

139 The Erlenmeyer flasks were constantly mixed on a magnetic stirring plate at 400 rpm
140 (Thermo Scientific, USA) in an incubation chamber (Snijders Scientific, The
141 Netherlands) controlled at 28°C. The light in the incubation chamber was provided by
142 14 fluorescent tubes at a total intensity of 17.9 W m⁻² (respectively 1.2, 13.8 and 2.8 W
143 m⁻² in the ranges 175-400, 400-700 and 700-1100 nm). All Erlenmeyer's were
144 randomized daily to provide an even distribution of light. During the experiment the
145 headspace was spiked with 80% H₂/20% N₂ when the gauge pressure dropped below +
146 0.1 bar (absolute pressure 1.1 bar).
147
148 Samples (3 mL) were taken axenically via the gas-tight septum after which the optical
149 density (OD), pH and temperature were measured instantly. The OD at 660 nm was
150 measured with an UV-VIS spectrophotometer (Shimadzu, Japan), while pH and
151 temperature were measured with a handheld device (Hanna Instruments, USA). A
152 maximum of 10 samples (30 mL or 10% of working volume) throughout the experiment
153 was taken to avoid disruption of the growth. After the determination of OD, pH and
154 temperature, samples were frozen (-20°C) for protein, fatty acids and pigments analysis.
155 Gas analysis and headspace pressure were monitored every 24 hours with respectively
156 gas chromatography and a manual manometer. At the end of the batch experiment (t=96
157 hours), samples of the broth were filtered (0.20 µm), to analyze the consumed total
158 ammoniacal nitrogen (NH₃ and NH₄⁺) in the medium with a San++Automated Wet
159 Chemistry analyzer (SkalarAnalytical, The Netherlands). Finally, samples (at t=0 and
160 t=96) for molecular analyses are kept at -80°C in case there is an indication of
161 contamination, as is closely monitored by verifying there are no shifts in the optical
162 density spectra during an incubation.

163 **2.4 BIOMASS GROWTH AND PRODUCTIVITY**

164 Bacterial growth (time vs. OD₆₆₀) was fitted via least squares regression to the Gompertz
 165 model modified by Zwietering *et al.* (1990) (time-derivative-type model) in GraphPad
 166 Prisma 8 software:

$$\ln\left(\frac{N_t}{N_0}\right) = \ln\left(\frac{N_m}{N_0}\right) * \exp\left[-\exp\frac{\mu_{max} * e}{\ln\left(\frac{N_m}{N_0}\right)} * (\lambda - t) + 1\right] \quad \text{Eq. 3}$$

167 in which N_t and N₀ are the biomass concentrations at time t and time 0, N_m is the
 168 maximum biomass concentration (reached at stationary phase), μ_{max} is the maximum
 169 specific growth rate, λ the lag time, and e the exponential constant (2.718). Maximum
 170 growth rates were, if needed, corrected to 28°C, based on an Arrhenius-type of equation
 171 assuming a doubling of activity from a temperature increase with 10°C.

172

173 The estimated total suspended solids (TSS) levels were based on OD₆₆₀-TSS
 174 correlations that were obtained prior to the detailed growth characterization:

175 *Rh. capsulatus*: $\frac{g\ DW}{L} = 433.34 * OD \quad R^2 = 0.94 \quad n=12$

176 *Rh. sphaeroides*: $\frac{g\ DW}{L} = 527.46 * OD \quad R^2 = 0.97 \quad n=12$

177 *Rps. palustris*: $\frac{g\ DW}{L} = 549.81 * OD \quad R^2 = 0.98 \quad n=12$

178 The TSS at different well distributed OD values (0.3, 0.6, 1.0 and 1.3) was determined
 179 in triplicate via the APHA methods 2540B and 2540D with Whatman® glass microfiber
 180 filters by diluting a batch culture at stationary phase. TSS productivities (g TSS L⁻¹ d⁻¹)
 181 were calculated in two ways, dividing the difference in TSS concentration X (g TSS L⁻¹)
 182 relatively to time point zero (overall productivity, t₀, X₀ → t_i, X_i) or between two time
 183 points (point-to-point productivity, t_{i-1}, X_{i-1} → t_i, X_i).

184 **2.5 HYDROGEN GAS CONSUMPTION AND DERIVED CALCULATIONS**

185 The percentage of hydrogen gas in the headspace was monitored by gas
186 chromatography (GC-2014) with argon gas as carrier, Shincarbon-ST 50/80 column and
187 TCD detection (shimadzu, Japan). The pressure in the Erlenmeyer flasks was monitored
188 with a manual manometer (Baumer, Germany). Hydrogen gas consumption in the
189 closed system was then calculated with the gas law and the biomass yield (g TSS g⁻¹ H₂)
190 was expressed as the net TSS produced to the hydrogen gas consumed.

191

192 The availability of dissolved hydrogen gas is an important factor to avoid growth
193 limitation of the purple bacteria. The saturation concentration of dissolved hydrogen gas
194 in the medium is reached when the pressure of the gas above the solution is equal to (i.e.
195 at equilibrium with) the pressure of the gas in the solution. To understand the potential
196 H₂ limitations, dissolved concentrations of hydrogen gas (C_{H₂}) were related to microbial
197 growth rates (μ) in the Monod equation (substrate-limiting-type model). This
198 mathematical model could indicate at which dissolved hydrogen concentrations
199 microbial growth would become limited.

200

201 Erlenmeyer flasks were set-up in the same manner as the batch growth test with partial
202 pressures of hydrogen (P_{H₂}) of 16, 32, 81, 97 and 103 kPa in a total pressure of 141 kPa,
203 which coincidences with dissolved hydrogen concentrations (C_{H₂}) of 0.25, 0.50, 1.25,
204 1.50 and 1.60 mg H₂ L⁻¹. This was done by flushing and spiking the headspace with
205 80% H₂/20% N₂ and 100% N₂ to reach the appropriate partial pressures. Dissolved
206 hydrogen concentrations were calculated as:

$$C_{H_2} = H * P_{H_2} * MM_{H_2} * 10^3 [mg H_2 L^{-1}] \quad \text{Eq. 4}$$

207 where H is the Henry constant of $7.7 \cdot 10^{-9} \text{ mol L}^{-1} \text{ Pa}^{-1}$ at 28°C (Fernández-Prini *et al.*
 208 2003), P_{H_2} the partial pressure of hydrogen gas in Pa and MM_{H_2} the molar mass of
 209 hydrogen gas. The saturation concentration ($C_{s_H_2}$) was taken as $1.6 \text{ mg H}_2 \text{ L}^{-1}$, which
 210 was previously found as the maximum solubility in water at 28°C at a P_{H_2} of 1 bar
 211 (Kolev 2011). Subsequently instantaneous growth rates (point-to-point, based on
 212 Gompertz growth model) were plotted against the dissolved H_2 concentration
 213 (normalized to atmospheric pressure) at each time point during the experiment.
 214 GraphPad Prisma 8 software was used to fit to the Monod model with least squares
 215 regression.

216
 217 Finally, the hydrogen gas utilization rate and the hydrogen gas supply rate were
 218 compared to rule out any hydrogen gas limitation during growth. The utilization rate
 219 was calculated as:

$$r_{H_2_demand} = \frac{-\mu * X}{Y_{biomass}} [mg H_2 L^{-1} d^{-1}] \quad \text{Eq. 5}$$

220 with μ the growth rate (d^{-1}), X the biomass concentration (mg TSS L^{-1}) and $Y_{biomass}$ the
 221 yield ($\text{g TSS g}^{-1} \text{ H}_2$). The supply rate was determined according to following equation:

$$r_{H_2_supply} = k_L a * (C_{s_H_2} - C_{H_2}) [mg H_2 L^{-1} d^{-1}] \quad \text{Eq. 6}$$

222 The volumetric mass transfer coefficient $k_L a$ is, among others, proportional to the
 223 square root of the diffusion coefficient D ($\text{m}^2 \text{ h}^{-1}$) of the H_2 . Due to the fast-and-easy
 224 determination of dissolved oxygen (DO) in the aqueous phase, the $k_L a$ for O_2 was
 225 determined as a proxy for the $k_L a$ of H_2 after which it was converted based on
 226 the sole difference in diffusion coefficients in the formula (at 25°C : $D_{O_2} = 2 \times 10^{-5} \text{ cm}^2 \text{ s}^{-1}$)

227 ¹; $D_{H_2} = 4.5 \times 10^{-5} \text{ cm}^2 \text{ s}^{-1}$). The transfer of H_2 is hence 1.5 times faster

228 than the O_2 transfer.

229

230 The k_{La} determination was performed in the Erlenmeyer flasks using the same growth
231 medium (section 2.2) and conditions (section 2.3) described earlier, but with two
232 important differences: (i) inoculum was not added to the (abiotic) flasks to avoid biotic
233 oxygen uptake, and (ii) the flasks were kept open to the atmosphere in the incubator to
234 enable the oxygen gas transfer. At the start of the experiment the medium was
235 chemically deoxygenated by adding sodium sulfite and cobalt (Ruchti *et al.* 1985). The
236 DO was measured with an electrode (Hach, USA) until the $C_{S_{O_2}}$ at this temperature
237 was reached. The k_{La} for oxygen was derived from the slope of the linearization of the
238 DO curve.

239 **2.6 PROTEIN QUANTITY, PRODUCTIVITY AND QUALITY**

240 Protein analysis was performed with a modified Lowry method (Markwell *et al.* 1978).

241 The biomass protein contents were expressed as fractions of the biomass (%TSS).

242 Protein productivities ($\text{g protein L}^{-1} \text{ d}^{-1}$) were calculated in two ways, dividing the
243 difference in protein concentration (g TSS L^{-1}) relatively to time point zero (overall
244 productivity, $t_0, X_0 \rightarrow t_i, X_i$) or between two time points (point-to-point productivity, $t_{i-1},$
245 $X_{i-1} \rightarrow t_i, X_i$).

246

247 Samples for total amino acid (TAA) analysis, and thus also essential amino acids
248 (EAA), were centrifuged ($5000 \times g$, 10 min), hydrolyzed (6M HCl, 110 °C, 24 h) with
249 vacuum and evaporated, after which the samples were re-dissolved in 0.75mM HCl and

250 stored at $-20\text{ }^{\circ}\text{C}$ before analysis. Cysteine, methionine and tryptophan could not be
 251 quantified with this type of hydrolyzation. The standard operating procedure of Agilent
 252 Technologies (Santa Clara, CA, USA) using ortho-phthalaldehyde (OPA)/9-
 253 fluorenylmethyl chloroformate (FMOC) derivatization was adopted, with separation
 254 using high pressure liquid chromatography and detection using a diode array detector
 255 (1290 Infinity II LC System, USA).

256

257 As a measure for protein quality, the essential amino acids found in the TAA analysis
 258 were used to express the dietary match. The protein quality (g EAA 100 g^{-1} protein) was
 259 expressed both on adapted Lowry or TAA protein content and a range of the quality was
 260 given:

$$Dietary\ match\ (\%) = \frac{EAA_{product} \left[\frac{g\ EAA}{100\ g\ protein} \right] * digestibility\ (\%)}{EAA_{required\ by\ organism} \left[\frac{g\ EAA}{100\ g\ protein} \right]} \quad Eq. 7$$

261 Three target organisms were chosen: humans, pigs and Penaeidae shrimp. As
 262 conventional and comparative protein sources meat (beef) (Gorissen and Witard 2018,
 263 Kashyap *et al.* 2018), soybean meal and fishmeal were taken (Heuzé V. 2020). The
 264 digestibility of the bacterial product was taken as 87.0% (Skrede *et al.* 2009).

265 Furthermore, the essential amino acids index (EAAI) was calculated based on the EAA
 266 content in the protein products compared to the EAA requirements (Oser 1959):

$$EAAI = \sqrt[n]{\frac{aa_1}{AA_1} * \frac{aa_2}{AA_2} * \dots * \frac{aa_n}{AA_n}} \quad Eq. 8$$

267 where n is the number of EAA, aa_n and AA_n are the EAA content in the protein product
 268 (g EAA g^{-1} protein) and EAA requirement of the organism (g EAA g^{-1} protein)
 269 respectively. The quality of the protein is classified according to the EAAI as superior

270 (>1), high (0.95-1), good (0.86-0.95), useful (0.75-0.86) or inadequate (<0.75) (Kent *et*
271 *al.* 2015).

272 **2.7 ADDITIONAL NUTRITIONAL PARAMETERS: FATTY ACIDS AND PIGMENTS**

273 Fatty acids (FA) methyl esters were prepared by direct esterification according to a
274 modified procedure (Lepage and Roy 1984) and identified with gas chromatography (Toi *et*
275 *al.* 2013). The bacteriochlorophyll a (Bchl a) and total carotenoid content were
276 determined by an acetone/methanol solvent (78:22 v/v) extraction, followed by
277 spectrophotometric analysis and conversion with the Lambert-Beer law (Liaaen-Jensen
278 and Jensen 1969, Brotosudarmo *et al.* 2015). Bacteriochlorophyll a has an extinction
279 coefficient of $65.3 \text{ mM}^{-1} \text{ cm}^{-1}$ at a wavelength of 771 nm (Brotosudarmo *et al.* 2015)
280 and a molar mass of 910.5 g/mol. For total carotenoids an average of $97.7 \text{ mM}^{-1} \text{ cm}^{-1}$ is
281 taken as extinction coefficients at the max absorbance between 475 and 525 nm with a
282 molar mass of 596 g/mol based on Liaaen-Jensen and Jensen (1969).

283 **2.8 STATISTICAL ANALYSES**

284 Statistical analyses were conducted in the program 'BM SPSS statistics 26'. One-way
285 ANOVA analyses compared means between objects. The normality of data residuals
286 was tested using the Shapiro-Wilk normality test. The assumption of homoscedasticity
287 was verified through a Levene's test. The Bonferroni post-hoc test was then used to
288 determine significant differences. The non-parametric Kruskal-Wallis rank sum test was
289 executed when normality was rejected. The Welch's t-test was used in case of
290 heteroscedasticity. Repeated measures ANOVA analysis was conducted to analyze
291 differences in results over time (dependent observations). Sphericity (compound

292 symmetry) of the data was tested with the Mauchly's Test and Bonferroni post-hoc
293 analysis gave the final results. A Greenhouse-Geisser correction was done if sphericity
294 was not met.

295 **3 RESULTS AND DISCUSSION**

296 **3.1 GROWTH KINETICS AND PROTEIN PRODUCTIVITY**

297 The growth curves of photohydrogenotrophic PB followed the conventional pattern of
298 lag, log and stationary phase (Figure 1A). With the modified Gompertz model (n=33)
299 maximum growth rates were calculated for *Rh. capsulatus*, *Rh sphaeroides* and *Rps.*
300 *palustris* and were respectively 2.70, 2.30 and 2.33 d⁻¹ (corrected to 28°C). A one-way
301 ANOVA confirmed that the μ_{\max} of *Rh. capsulatus* was significantly higher ($p<0.05$)
302 than *Rh. sphaeroides* and *Rps. palustris*. The difference between the latter two was not
303 significant. The difference between the latter two was not significant. It should be noted
304 that the growth stage and activity of the inoculum used (taken from the exponential
305 phase here) may have had a positive impact on the achievable μ_{\max} . This is of relevance
306 for the results in section 3.3 below, where a *Rh. capsulatus* inoculum from the late
307 stationary phase yielded a lower μ_{\max} .

308
309 Extrapolating and benchmarking growth rates, sometimes obtained under different
310 growth conditions, should be carefully done, yet enables to judge application potential.
311 The maximum growth rates obtained (2.30-2.70 d⁻¹) were in line with
312 photohydrogenotrophic growth rates found in literature, ranging from 0.3 to 3.8 d⁻¹ (at
313 28°C) (Douthit and Pfennig 1976, Rey *et al.* 2006), and could hence be higher than
314 microalgal growth rates (0.3-2.4 d⁻¹ at 28°C) (Lakaniemi *et al.* 2012, Sunjin Kim 2013,

315 Sui and Vlaeminck 2018, Sui *et al.* 2019). However, compared to photoheterotrophic
316 purple bacteria ($0.5-7.2\text{ d}^{-1}$ at 28°C) (Vrati 1984, Willison 1988, Alloul *et al.* 2019) and
317 HOB ($1.5-8.8\text{ d}^{-1}$ at 28°C) (Ishizaki and Tanaka 1990, Matassa *et al.* 2016), the μ_{max}
318 obtained under photohydrogenotrophy was in the lower range.

319

320 A repeated measures ANOVA with a Greenhouse-Geisser correction determined that
321 mean protein contents did not differ significantly ($p<0.05$) along the growth phases
322 (Figure 1C). The average protein content over the whole batch experiment for *Rh.*
323 *capsulatus*, *Rh. sphaeroides* and *Rps. palustris* were respectively 50.9%, 41.5% and
324 37.9%. These protein contents did differ significantly ($p<0.05$) with *Rh. capsulatus*
325 achieving the highest protein content. At the end of the batch experiment $74-85\text{ mg N L}^{-1}$
326 ¹ has been consumed from the initially provided N in the medium (310 mg N L^{-1}).

327 Applying the generic protein-to-nitrogen conversion factor of 6.25 on the achieved
328 protein contents in the PB, 50-66% of this N consumption can be attributed to protein
329 production. The remaining N consumption could be attributed to nucleic acid content
330 (typically 30-38% of N in biomass) (Bruce and Perry 2001), Bchl a content (typically
331 0.2-0.5% of N in biomass) or to the possible stripping of NH_3 to the headspace.

332

333 Furthermore, it is seen that the maximal productivities coincides with the early
334 stationary growth phase (Figure 1B). No significant differences ($p<0.05$) were found in
335 the TSS productivities (overall and point-to-point) over time for a specific species or
336 between species at the same time point. The overall and point-to-point protein
337 productivities shown in Figure 1D correspond with maximum productivities of 0.09-
338 0.12 and 0.16-0.22 $\text{g protein L}^{-1}\text{ d}^{-1}$ and show the same trends as the TSS productivities

339 (Figure 1B). The maximum TSS and protein productivities coincides, as expected, since
340 the protein content does not differ significantly over time. And thus, again, the maximal
341 values are at the start of the stationary phase.

342

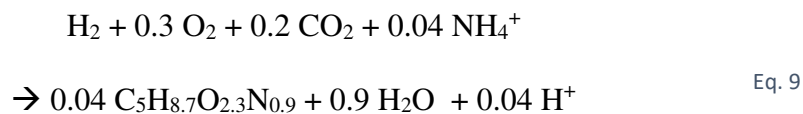
343 As previously stated, no nutritional data of photohydrogenotrophically grown PB are
344 available. Therefore, microbial protein sources that express metabolic similarities with
345 the photohydrogenotrophic purple bacteria were selected to enable comparison within
346 the field. Most often, protein productivity is expressed as crude protein in literature,
347 which is the nitrogen content multiplied by a factor 6.25, and results in an
348 overestimation of the total protein content. Therefore protein data measured with the
349 adapted Lowry or TAA method, were converted to crude protein by applying a
350 conversion ratio of 1.31 and 1.33 respectively (Muys *et al.* 2019). Based on the average
351 protein productivities (Figure 2), the photohydrogenotrophic PB in this study are 1.5
352 times faster than microalgae (0.02-0.19 g protein L⁻¹ d⁻¹) (Ogbonda *et al.* 2007, Hempel
353 *et al.* 2012, Sui and Vlaeminck 2018), but 4.4 times slower than photoheterotrophic
354 purple bacteria (0.22-0.84 g protein L⁻¹ d⁻¹) (Alloul *et al.* 2019, Capson-Tojo *et al.*
355 2020). As expected, the phototrophic protein productivities are well below those of
356 aerobic chemotrophic HOB (1.2-13.1 g protein L⁻¹ d⁻¹) (Ishizaki and Tanaka 1990,
357 Matassa *et al.* 2016), due to the difference in energy source (phototrophic versus aerobic
358 hydrogen oxidation) (Schmidt-Rohr 2020)

359 **3.2 H₂-BASED BIOMASS AND PROTEIN YIELDS**

360 The biomass yields in the batch experiment were respectively 5.1, 6.7 and 7.8 g TSS g⁻¹
361 H₂ for *Rh. capsulatus*, *Rh. sphaeroides* and *Rps. palustris* at the stationary phase (Figure

362 3A). The expected biomass yield of purple bacteria, based on the stoichiometry (Eq. 2),
 363 was 7.0 g TSS g⁻¹ H₂. For this, a similar ratio of 0.8 for volatile suspended solids over
 364 TSS was used as observed in photoheterotrophically grown PNSB (Alloul *et al.* 2019),
 365 with likely phosphorus as important inorganic biomass constituent, not only bound in
 366 organic molecules but also stored as polyphosphate (Sakarika *et al.* 2020). Statistical
 367 analysis showed that the biomass yield of *Rps. palustris* was significantly higher
 368 (*p*<0.05) than *Rh. capsulatus*, but no significant difference with *Rh. sphaeroides* was
 369 found. The protein yield was similarly plotted in Figure 3B and considers the protein
 370 content of the three PB species. Contrary to biomass yield, no significant differences
 371 were found between species, with values of 2.6, 2.9 and 2.8 g protein g⁻¹ H₂. *Rh.*
 372 *capsulatus* is able to compensate its lower biomass yield with a significantly higher
 373 protein content as seen in Figure 1C.

374 The biomass and protein yields were promising compared to the lower yields of
 375 hydrogen oxidizing bacteria, which could be expected based on their stoichiometry
 376 (stoichiometry of Matassa *et al.* (2016) was adapted to include biomass as
 377 C₅H_{8.7}O_{2.3}N_{0.9}):



378 resulting in a biomass yield of 2.8 g TSS g⁻¹ H₂ (a ratio of 0.8 is assumed for volatile
 379 suspended solids over TSS). Actual empirical data for HOB biomass and protein yields
 380 found in literature amount to 0.6-2.4 g TSS g⁻¹ H₂ and 0.4-1.7 g protein g⁻¹ H₂ on
 381 average respectively (Ishizaki and Tanaka 1990, Matassa *et al.* 2016). On average, the
 382 photohydrogenotrophic PB were thus able to utilize hydrogen gas 3.4 and 2.3 times
 383 more efficient for biomass and protein production compared to HOB.

384 **3.3 HYDROGEN GAS AVAILABILITY**

385 To rule out any growth limitation due to H₂ availability, a comparison of H₂ supply and
386 uptake rates were made. The Monod relationship (Figure 4A) related the microbial
387 maximum growth rates with the availability of estimated dissolved hydrogen levels. A
388 maximum specific growth rate of 2.12 d⁻¹ was found and a half velocity constant K_s of
389 0.17 mg H₂ L⁻¹ (R²=0.88). The activity of the *Rh. capsulatus* inoculum (late stationary
390 phase) of this series of batch experiments was lower and thus resulted in a lower μ_{max}
391 compared to section 3.1. However, the achieved μ_{max} of *Rh. capsulatus* in section 3.1
392 was in the same order of magnitude as the two other PB species, which provides
393 confidence in the validity of these results.

394 Nevertheless, the results still represent a good proxy for limiting hydrogen
395 concentrations. The low value of K_s shows that the growth rate increases rapidly at low
396 aqueous hydrogen gas concentrations. The long-lasting plateau enhances this feature, as
397 still 82% of the maximum growth rate is achieved at half of the saturation concentration
398 of hydrogen gas (0.8 mg H₂ L⁻¹).

399

400 Additionally, as gas measurements are time consuming, it was determined whether
401 pressure drop could be used as a proxy for hydrogen gas consumption. The expected
402 pressure drop is calculated by substituting the measured H₂ consumption as follows:

$$\frac{\Delta P}{\Delta m} = \frac{R * T}{MM * V * Vol\%} = 5.04 \quad \text{Eq. 10}$$

403 In which it was assumed that the gas composition is fixed (80 vol%-H₂). The
404 nonparametric spearman correlation coefficient between the expected and empirical

405 pressure drops is 0.85. The empirical pressure drop could thus act as a fast proxy for
406 hydrogen gas consumption. The gap between the expected and empirical value can be
407 explained by the gas composition changes. Due to the release of CO₂ to the headspace,
408 via the equilibrium CO₂/HCO₃⁻/CO₃²⁻, the volume percentage of H₂ in the headspace is
409 not fixed.

410

411 The mass transfer coefficient of oxygen was determined in the Erlenmeyer flasks and
412 found to be 32.65 d⁻¹. Applying the conversion factor of 1.5, a K_{LA} of 48.97 d⁻¹ was
413 found for hydrogen gas. The maximum supply rate of hydrogen gas could then be
414 calculated as 78.36 mg H₂ L⁻¹ d⁻¹ if the saturation concentration is taken as 1.6 mg H₂ L⁻¹.
415 ¹. The hydrogen gas demand rate was plotted for the three PB species in Figure 4B over
416 the course of the batch experiment and showed that no H₂ flux limitation occurred
417 during growth.

418 **3.4 NUTRITIONAL PROFILE: AMINO ACIDS, FATTY ACIDS AND PIGMENTS**

419 The TAA content was quantified at 96 hours in the stationary phase for each species.
420 The applied hydrolyzation on the biomass, destroys the amino acids cysteine,
421 methionine and tryptophan, and thus will result in an underestimation of the TAA.
422 Overall, the *Rhodobacter* species are showing higher TAA content in the TSS, which is
423 similar to what was found with the adapted Lowry method for protein content
424 determination (Figure 1C).

425

426 Compared with the adapted Lowry method, the ratio of Lowry-protein over TAA is
427 1.19, 1.08 and 1.13 for *Rh. capsulatus*, *Rh. sphaeroides* and *Rps. palustris* respectively.

428 The adapted Lowry method overestimates the total protein content of the PB biomass by
429 an average of 13.5%. However, the adapted Lowry method allows for a fast
430 determination of protein content with a low quantity of sample needed. Furthermore,
431 feed and food industries mostly communicate protein content as crude protein (based on
432 N measurements), which even overestimates the protein content up to 31% (Muys *et al.*
433 2019).

434

435 The content of EAA is more important for the food and feed industry as these cannot be
436 synthesized by our target organisms and must be obtained from feed or food. The nine
437 EAA are: histidine, isoleucine, leucine, lysine, methionine/cysteine,
438 phenylalanine/tyrosine, tryptophan, threonine and valine. The total amount of EAA in
439 the biomass accounts for 37.5, 42.5 and 41.8 % of the TAA for *Rh. capsulatus*, *Rh.*
440 *sphaeroides* and *Rps. palustris* respectively (Figure 5A). Differences in the profile can
441 be visually distinguished, however, no statistical analysis was performed due to the low
442 number of observations (n=2).

443

444 The dietary match between the three PB species and the human needs was expressed as
445 a min-max range (Figure 5B). The adapted Lowry method often overestimates the true
446 protein content in the biomass, and thus is linked to the minima of the range, while the
447 TAA method, linked to the maxima, gives a slight underestimation, since the applied
448 hydrolysis was unable to quantify three amino acids. It is seen that all PB species are
449 able to fulfill all dietary needs for humans. The dietary match of beef is often the
450 highest, but it is important to note that everything above 100% match will not
451 increasingly add in nutritional quality, as this excess in AA will not be taken up. The

452 dietary match for pigs and penaeidae shrimp have more variable outcomes. However, it
453 is noteworthy that the photohydrogenotrophic PB show a similar protein quality
454 compared to the conventional feed protein sources soybean meal and fishmeal.
455

456 Lastly, Figure 5C shows the EAAI for all target organisms with the PB and
457 conventional protein sources. All EAAI are above 0.75 and thus all PB are adequate
458 candidates as a protein replacement. It is confirmed that all PB species are of superior
459 quality for human food consumption as a protein replacement. Moreover, *Rh.*
460 *capsulatus* showed the highest potential, reaching respectively high and superior protein
461 quality for pigs and penaeidae shrimp according to the EAAI scale (Kent *et al.* 2015).
462 On the other side of the nutritional spectrum, the fatty acid content and composition of
463 each PB is shown in Figure 6. Fatty acids are a major source of energy and can be
464 subdivided in saturated (no double C-C bonds) and unsaturated (mono or poly, which
465 have respectively 1 or more double C-C bonds). Total FA content in the biomass is 6.8,
466 7.1 and 6.1 g FA 100 g⁻¹ TSS respectively for *Rh. capsulatus*, *Rh. sphaeroides* and *Rps.*
467 *palustris*. Microalgae contain FA in the same order of magnitude (7.2 g FA 100 g⁻¹
468 TSS), but with a high composition of saturated fatty acids (39%) (Ortega-Calvo *et al.*
469 1993, Suh *et al.* 2015). Figure 6 shows that the FA profile is dominated by
470 monosaturated FA (91%), with a low amount of saturated FA (7%). The dietary
471 guidelines recommend reducing the intake of saturated fatty acids to reduce the
472 cholesterol levels and thus the risk of cardiovascular disease.
473

474 Interestingly, the results showed high amounts of vaccenic acid (82-86% of total fatty
475 acid content), which is an unambiguous marker of purple bacteria (Imhoff 1991). This is

476 of great importance since vaccenic acid can have a beneficial effect on human health
477 (Field *et al.* 2009). Essential fatty acids, linoleic and α -linolenic, which can be used as
478 precursors to generate a range of fatty acids (Scientific Advisory Committee on
479 Nutrition 2018) were not detected in the three photohydrogenotrophically grown PB.

480

481 Lastly, the main pigments, Bchl a, and carotenoids were determined for *Rh. capsulatus*,
482 *Rh. sphaeroides* and *Rps. palustris*. Both pigments possess antioxidant properties, while
483 carotenoids can decrease the risk of certain cancers and eye diseases for humans
484 (George *et al.* 2020). No significant differences were found between species for both
485 pigments. Bacteriochlorophyll a content in the photohydrogenotrophic PB (0.3-0.6
486 %TSS) was lower compared to levels found in photoheterotrophic PB of 0.7-1.7 %TSS
487 (Alloul *et al.* 2020). Carotenoids, on the other hand, were in the higher range (0.3-0.4
488 %TSS) of values found in literature for photoheterotrophic PB (0.05-0.4 %TSS)
489 (Capson-Tojo *et al.* 2020).

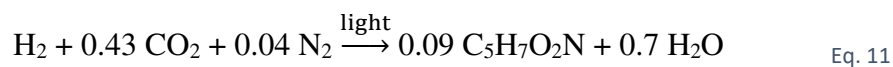
490 **3.5 OUTLOOK**

491 Depending on the chosen source(s) of the sustainable resources (energy, H₂, CO₂,
492 nitrogen, phosphorus,...), the proposed cleantech process can fit in one or more
493 upcoming sustainable economy concepts: the hydrogen economy, the bioeconomy and
494 the circular economy. Microbial food production based on renewable and/or recovered
495 resources with minimal requirement of arable land and fossil-based resources has an
496 excellent environmental sustainability potential. Besides the resource origin options
497 listed in the introduction, an appealing additional option to consider is N₂ as nitrogen
498 source. Purple bacteria are capable of N₂ fixation (George *et al.* 2020), and exploiting

499 this feature could avoid the environmental footprint from synthetic N fertilizer
500 production or from a nitrogen recovery process. The questions to be investigated
501 include the impact of a slightly higher H₂ requirement and hence lower H₂-to-biomass
502 yield, and a potential decrease of the growth rate (and hence protein productivity), both
503 of which were observed previously for HOB (Hu *et al.* 2020).

504

505 Furthermore, the choice of carbon and nitrogen source will also have its effect on the pH
506 control strategy. The stoichiometric equations show the impact of the C species on the
507 pH, with a moderate alkalization using mainly bicarbonate (−0.3 mol H⁺ mol^{−1} H₂) (Eq.
508 2) versus a slight acidification based on CO₂ (+0.1 mol H⁺ mol^{−1} H₂) (Eq. 1). Furthermore,
509 using a gaseous N source further affects the balance, with no net pH change
510 stoichiometrically expected based on N₂ dosage:



511 While these assumptions still require experimental validations and additional metabolic
512 pathways may influence the final outcome, pH control based on CO₂ dosage could be an
513 option.

514

515 Looking ahead, a major next research challenge for this concept of microbial food
516 production is intensification in a bioreactor, which will be linked to minimizing H₂ and
517 light limitations, through efficient gas-to-liquid (G-to-L) transfer and supply of light,
518 respectively. Fortunately, both aspects are individually approached in the parallel
519 research, development and innovation activities of two other types of MP or microbial
520 biomass: HOB and microalgae (in closed photobioreactors), respectively. Therefore, the

521 challenge moves to integrating the ‘best of both worlds’, and balance the availability of
522 H₂ and light.
523 HOB production is currently at the stage of industrial validation with microbial products
524 such as Solein, Novomeal and Proton (Alloul *et al.* 2021). Of particular interest here is
525 that the biomass and protein yields of photohydrogenotrophic PB are significantly
526 higher than for HOB, which in combination with their lower growth rates and biomass
527 levels leads to a considerable 142 times lower volumetric H₂ demand rate (Ishizaki and
528 Tanaka 1990, Matassa *et al.* 2016). Therefore, adopting similar G-to-L transfer
529 approaches should be more than sufficient to avoid limitations. Microalgae production
530 in closed photobioreactors is already at the level of industrial demonstration and
531 commercialization with products such as NannoPrime (Proviron) and *Chlorella vulgaris*
532 (Algomed). Insights in optimizing light distribution, proper mixing and the energy need
533 in such photobioreactors can be used (Posten 2009).

534 **4 CONCLUSIONS**

535 Among the photoautotrophs, the three tested species (*Rh. capsulatus*, *Rh. sphaeroides*
536 and *Rps. palustris*) obtained promising growth rates (2.3-2.7 d⁻¹ at 28°C) and protein
537 productivities (0.09-0.12 g protein L⁻¹ d⁻¹), exhibiting likely faster and more productive
538 characteristics than microalgae. Biomass and protein yields (2.6-2.9 g protein g⁻¹ H₂)
539 transcended the ones of aerobic hydrogen oxidizing bacteria by respectively a factor of
540 3.4 and 2.3, rendering a more resource-friendly MP production. The three species
541 provided a superior protein quality for human dietary needs and vaccenic acid, likely
542 beneficial for humans, was found in high amounts (82-86% of total fatty acid content).
543

544 E-supplementary data of this work can be found in e-version of this paper online

545 **5 REFERENCES**

- 546 1 Alloul, A., M. Cerruti, D. Adamczyk, D. G. Weissbrodt and S. E. Vlaeminck
547 (2020). "Control tools to selectively produce purple bacteria for microbial protein in
548 raceway reactors." bioRxiv 912980 [preprint].
549
- 550 2 Alloul, A., J. Spanoghe, D. Machado and S. E. Vlaeminck (2021). "Unlocking the
551 genomic potential of aerobes and phototrophs for the production of nutritious and
552 palatable microbial food without arable land or fossil fuels." *Microb Biotechnol.*
553
- 554 3 Alloul, A., S. Wuyts, S. Lebeer and S. E. Vlaeminck (2019). "Volatile fatty acids
555 impacting phototrophic growth kinetics of purple bacteria: Paving the way for protein
556 production on fermented wastewater." *Water Research* **152**: 138-147.
557
- 558 4 Boland, M. J., A. N. Rae, J. M. Vereijken, M. P. M. Meuwissen, A. R. H. Fischer,
559 M. A. J. S. van Boekel, S. M. Rutherford, H. Gruppen, P. J. Moughan and W. H. Hendriks
560 (2013). "The future supply of animal-derived protein for human consumption." *Trends in*
561 *Food Science & Technology* **29**: 62-73.
562
- 563 5 Brotosudarmo, T. H. P., L. Limantara, Heriyanto and M. N. U. Prihastyanti
564 (2015). "Adaptation of the Photosynthetic Unit of Purple Bacteria to Changes of Light
565 Illumination Intensities." *Procedia Chemistry* **14**: 414-421.
566
- 567 6 Bruce, E. R. and L. M. Perry (2001). *Environmental Biotechnology: Principles*
568 *and Applications*. New York, McGraw-Hill Education.
569
- 570 7 Campbell, B. M., D. J. Beare, E. M. Bennett, J. M. Hall-Spencer, J. S. I. Ingram,
571 F. Jaramillo, R. Ortiz, N. Ramankutty, J. A. Sayer and D. Shindell (2017). "Agriculture
572 production as a major driver of the earth system exceeding planetary boundaries."
573 *Ecology and Society* **22**.
574
- 575 8 Capson-Tojo, G., D. J. Batstone, M. Grassino, S. E. Vlaeminck, D. Puyol, W.
576 Verstraete, R. Kleerebezem, A. Oehmen, A. Ghimire, I. Pikaar, J. M. Lema and T. Hulsen
577 (2020). "Purple phototrophic bacteria for resource recovery: Challenges and
578 opportunities." *Biotechnol Adv*: 107567.
579
- 580 9 Colbeau, A., B. C. Kelley and P. M. Vignais (1980). "Hydrogenase Activity in
581 *Rhodospseudomonas capsulata*: Relationship with Nitrogenase Activity." *Journal of*
582 *bacteriology* **144**: 141-148.
583
- 584 10 Douthit, H. A. and N. Pfennig (1976). "Isolation and growth rates of Methanol
585 utilizing *Rhodospirillaceae*." *Archives of Microbiology* **107**: 233-234.
586
- 587 11 Fernández-Prini, R., J. L. Alvarez and A. H. Harvey (2003). "Henry's Constants
588 and Vapor-Liquid Distribution Constants for Gaseous Solutes in H₂O and D₂O at High
589 Temperatures." *Journal of Physical and Chemical Reference Data* **32**(2): 903-916.
590

- 591 12 Field, C. J., H. H. Blewett, S. Proctor and D. Vine (2009). "Human health benefits
592 of vaccenic acid." *Appl Physiol Nutr Metab* **34**(5): 979-991.
593
- 594 13 George, D. M., A. S. Vincent and H. R. Mackey (2020). "An overview of
595 anoxygenic phototrophic bacteria and their applications in environmental biotechnology
596 for sustainable Resource recovery." *Biotechnol Rep (Amst)* **28**: e00563.
597
- 598 14 Gorissen, S. H. M. and O. C. Witard (2018). "Characterising the muscle anabolic
599 potential of dairy, meat and plant-based protein sources in older adults." *Proc Nutr Soc*
600 **77**(1): 20-31.
601
- 602 15 Hempel, N., I. Petrick and F. Behrendt (2012). "Biomass productivity and
603 productivity of fatty acids and amino acids of microalgae strains as key characteristics of
604 suitability for biodiesel production." *J Appl Phycol* **24**(6): 1407-1418.
605
- 606 16 Heuzé V., T. G., Kaushik S., (2020, 11/5/2015). "Feedipedia, a programme by
607 INRA, CIRAD, AFZ and FAO.", from <https://www.feedipedia.org>.
608
- 609 17 Hu, X., F. M. Kerckhof, J. Ghesquiere, K. Bernaerts, P. Boeckx, P. Clauwaert and
610 N. Boon (2020). "Microbial Protein out of Thin Air: Fixation of Nitrogen Gas by an
611 Autotrophic Hydrogen-Oxidizing Bacterial Enrichment." *Environ Sci Technol* **54**(6):
612 3609-3617.
613
- 614 18 Imhoff, J. F. (1991). "Polar Lipids and Fatty Acids in the Genus *Rhodobacter*."
615 *Systematic and Applied Microbiology* **14**(3): 228-234.
616
- 617 19 Ishizaki, A. and K. Tanaka (1990). Batch Culture of *Alcaligenes eutrophus* ATCC
618 17697 T Using Recycled Gas Closed Circuit Culture System. *Journal of fermentation and*
619 *bioengineering*.
620
- 621 20 Kashyap, S., N. Shivakumar, A. Varkey, R. Duraisamy, T. Thomas, T. Preston,
622 S. Devi and A. V. Kurpad (2018). "Ileal digestibility of intrinsically labeled hen's egg and
623 meat protein determined with the dual stable isotope tracer method in Indian adults." *Am*
624 *J Clin Nutr* **108**(5): 980-987.
625
- 626 21 Kent, M., H. M. Welladsen, A. Mangott and Y. Li (2015). "Nutritional evaluation
627 of Australian microalgae as potential human health supplements." *PLoS One* **10**(2):
628 e0118985.
629
- 630 22 Kolev, N. I. (2011). Solubility of O₂, N₂, H₂ and CO₂ in water. *Multiphase Flow*
631 *Dynamics* **4**: 209-239.
632
- 633 23 Lakaniemi, A. M., V. M. Intihar, O. H. Tuovinen and J. A. Puhakka (2012).
634 "Growth of *Chlorella vulgaris* and associated bacteria in photobioreactors." *Microb*
635 *Biotechnol* **5**(1): 69-78.
636

637 24 Lepage, G. and C. C. Roy (1984). "Improved recovery of fatty acid through direct
638 transesterification without prior extraction or purification." *Journal of lipid research* **25**:
639 1391-1396.

640

641 25 Liaaen-Jensen, S. and A. Jensen (1969). "Quantitative Determination of
642 Carotenoids in Photosynthetic Tissues." **294**: 586-602.

643

644 26 Madigan, M. T. and H. Gest (1979). "Growth of the Photosynthetic Bacterium
645 *Rhodospseudomonas capsulata* Chemoautotrophically in Darkness with H₂ as the Energy
646 Source." *Journal of bacteriology* **137**: 524-530.

647

648 27 Markwell, M. A. K., S. M. Haas, L. L. Bieber and N. E. Tolbert (1978). "A
649 modification of the Lowry procedure to simplify protein determination in membrane and
650 lipoprotein samples." *Analytical Biochemistry* **87**(1): 206-210.

651

652 28 Matassa, S., W. Verstraete, I. Pikaar and N. Boon (2016). "Autotrophic nitrogen
653 assimilation and carbon capture for microbial protein production by a novel enrichment
654 of hydrogen-oxidizing bacteria." *Water Research* **101**: 137-146.

655

656 29 Muys, M., Y. Sui, B. Schwaiger, C. Lesueur, D. Vandenneuvel, P. Vermeir and
657 S. E. Vlaeminck (2019). "High variability in nutritional value and safety of commercially
658 available *Chlorella* and *Spirulina* biomass indicates the need for smart production
659 strategies." *Bioresource Technology* **275**: 247-257.

660

661 30 Ogbonda, K. H., R. E. Aminigo and G. O. Abu (2007). "Influence of temperature
662 and pH on biomass production and protein biosynthesis in a putative *Spirulina* sp."
663 *Bioresource Technology* **98**: 2207-2211.

664

665 31 Ortega-Calvo, J. J., C. Mazuelos, B. Hermosin and C. Saiz-Jimenez (1993).
666 "Chemical composition of *Spirulina* and eukaryotic algae food products marketed in
667 Spain." *Journal of Applied Phycology* **5**: 425-435.

668

669 32 Oser, B. L. (1959). *An Integrated Essential Amino Acid Index for Predicting the
670 Biological Value of Proteins. Protein and Amino Acid Nutrition.* A. A. Albanese. New
671 York, Academic Press: 281-295.

672

673 33 Pikaar, I., S. Matassa, B. L. Bodirsky, I. Weindl, F. Humpenöder, K. Rabaey, N.
674 Boon, M. Bruschi, Z. Yuan, H. van Zanten, M. Herrero, W. Verstraete and A. Popp
675 (2018). "Decoupling Livestock from Land Use through Industrial Feed Production
676 Pathways." *Environmental Science & Technology* **52**: 7351-7359.

677

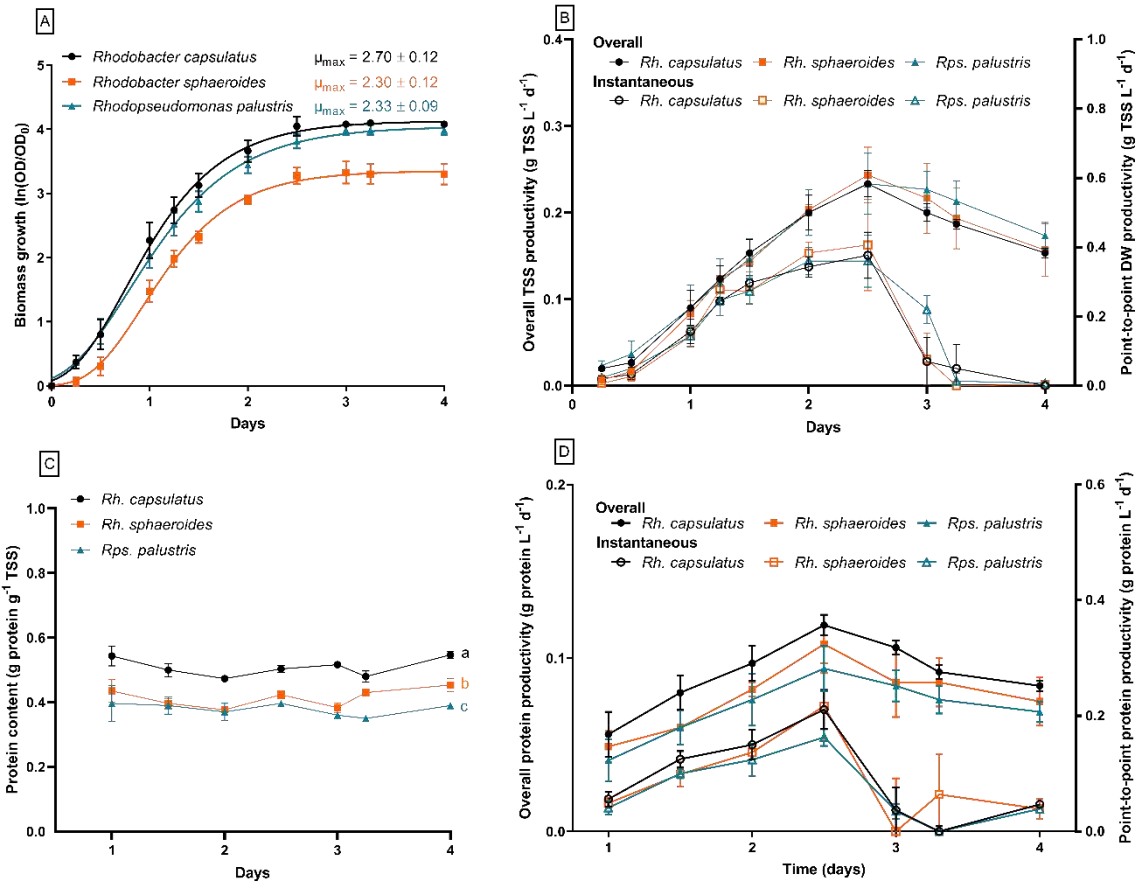
678 34 Posten, C. (2009). "Design principles of photo-bioreactors for cultivation of
679 microalgae." *Engineering in Life Sciences* **9**(3): 165-177.

680

681 35 Rey, F. E., Y. Oda and C. S. Harwood (2006). "Regulation of Uptake
682 Hydrogenase and Effects of Hydrogen Utilization on Gene Expression in
683 *Rhodospseudomonas palustris*." *Journal of bacteriology* **188**: 6143-6152.

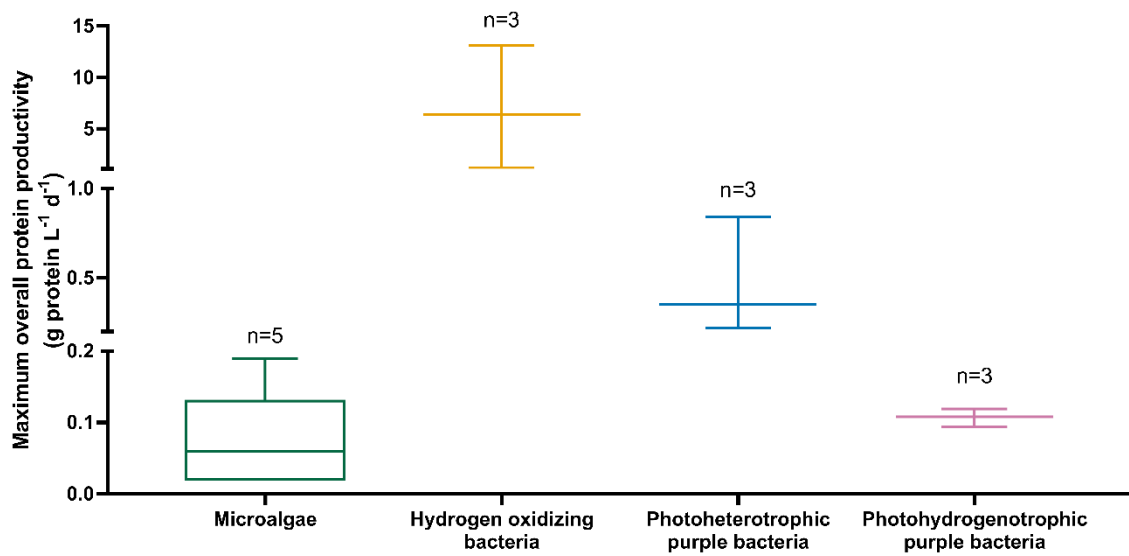
684
685 36 Ruchti, G., I. J. Dunn and J. R. Bourne (1985). "Practical Guidelines for the
686 Determination of Oxygen Transfer Coefficients (K_a) with the Sulfite Oxidation
687 Method." *The Chemical Engineering Journal* **30**: 29-38.
688
689 37 Sakarika, M., J. Spanoghe, Y. Sui, E. Wambacq, O. Grunert, G. Haesaert, M.
690 Spiller and S. E. Vlaeminck (2020). "Purple non-sulphur bacteria and plant production:
691 benefits for fertilization, stress resistance and the environment." *Microb Biotechnol*
692 [preprint].
693
694 38 Schmidt-Rohr, K. (2020). "Oxygen Is the High-Energy Molecule Powering
695 Complex Multicellular Life: Fundamental Corrections to Traditional Bioenergetics."
696 *ACS Omega* **5**(5): 2221-2233.
697
698 39 Scientific Advisory Committee on Nutrition (2018). Saturated fats and health:
699 233.
700
701
702 40 Skrede, A., L. Mydland and M. Øverland (2009). "Effects of growth substrate and
703 partial removal of nucleic acids in the production of bacterial protein meal on amino acid
704 profile and digestibility in mink." *Journal of Animal and Feed Sciences* **18**: 689-698.
705
706 41 Suh, S.-S., S. J. Kim, J. Hwang, M. Park, T.-K. Lee, E.-J. Kil and S. Lee (2015).
707 "Fatty acid methyl ester profiles and nutritive values of 20 marine microalgae in Korea."
708 *Asian Pacific Journal of Tropical Medicine* **8**(3): 191-196.
709
710 42 Sui, Y., M. Muys, D. B. Van de Waal, S. D'Adamo, P. Vermeir, T. V. Fernandes
711 and S. E. Vlaeminck (2019). "Enhancement of co-production of nutritional protein and
712 carotenoids in *Dunaliella salina* using a two-phase cultivation assisted by nitrogen level
713 and light intensity." *Bioresource Technology* **287**: 121398.
714
715 43 Sui, Y., M. Muys, P. Vermeir, S. D'Adamo and S. E. Vlaeminck (2019). "Light
716 regime and growth phase affect the microalgal production of protein quantity and quality
717 with *Dunaliella salina*." *Bioresource Technology* **275**: 145-152.
718
719 44 Sui, Y. and S. E. Vlaeminck (2018). "Effects of salinity, pH and growth phase on
720 the protein productivity by *Dunaliella salina*."
721
722 45 Sunjin Kim, J.-e. P., Yong-Beom Cho, Sun-Jin Hwang (2013). "Growth rate,
723 organic carbon and nutrient removal rates of *Chlorella sorokiniana* in autotrophic,
724 heterotrophic and mixotrophic conditions." *Bioresour Technol* **144**: 8-13.
725
726 46 Toi, H. T., P. Boeckx, P. Sorgeloos, P. Bossier and G. Van Stappen (2013).
727 "Bacteria contribute to *Artemia* nutrition in algae-limited conditions: A laboratory study."
728 *Aquaculture* **388-391**: 1-7.
729

- 730 47 Vratsi, S. (1984). "Single cell protein production by photosynthetic bacteria grown
731 on the clarified effluents of biogas plant." *Applied Microbiology and Biotechnology*
732 **19**(3): 199-202.
733
- 734 48 Wang, X., H. V. Modak and F. R. Tabita (1993). "Photolithoautotrophic Growth
735 and Control of CO₂ Fixation in *Rhodobacter sphaeroides* and *Rhodospirillum rubrum* in
736 the Absence of Ribulose Bisphosphate Carboxylase-Oxygenase." *Journal of Bacteriology*
737 **175**: 7109-7114.
738
- 739 49 Willison, J. C. (1988). "Pyruvate and Acetate Metabolism in the Photosynthetic
740 Bacterium *Rhodobacter capsulatus*." *Journal of General Microbiology* **134**: 2429-2439.
741
- 742 50 Zwietering, M. H., I. Jongenburger, F. M. Rombouts, K. Van ' and T. Riet (1990).
743 "Modeling of the Bacterial Growth Curve." *Applied and environmental microbiology* **56**:
744 1875-1881.
745



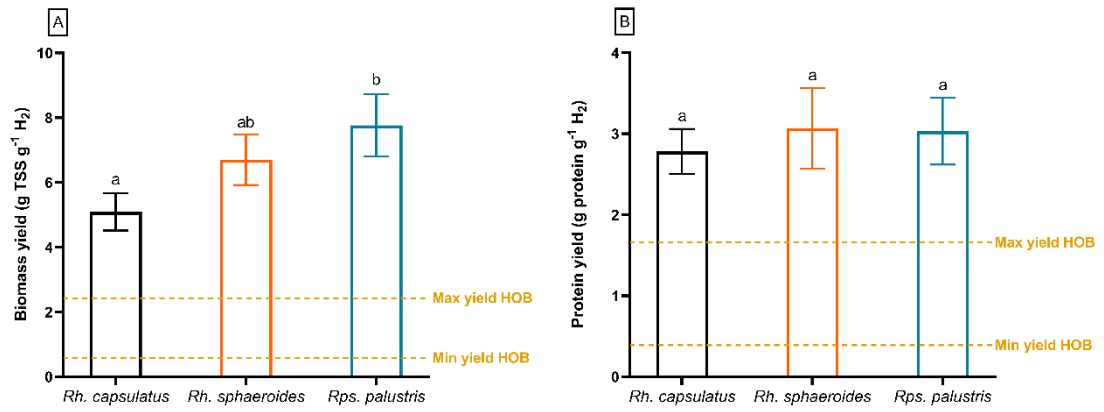
747

748 Figure 1: Growth curves of *Rh. capsulatus*, *Rh. sphaeroides* and *Rps. palustris* (panel A) with the modified Gompertz
 749 model based on the optical density data over time (n=3 per time point, n=33 for model). Overall and point-to-point
 750 total suspended solids (TSS) productivities over the time of the batch experiment (panel B). If the point-to-point
 751 productivity was negative, it was set at zero. Each data point shows the average and standard deviation (n=3).
 752 Protein content over time for *Rhodobacter capsulatus*, *Rhodobacter sphaeroides* and *Rhodopseudomonas palustris*
 753 (panel C) and overall and point-to-point protein productivities over the time of the batch experiment (panel D). If
 754 the point-to-point productivity was negative, it was set at zero. Each data point shows the average and standard
 755 deviation (n=3). Letters denote significant differences ($p < 0.05$).
 756



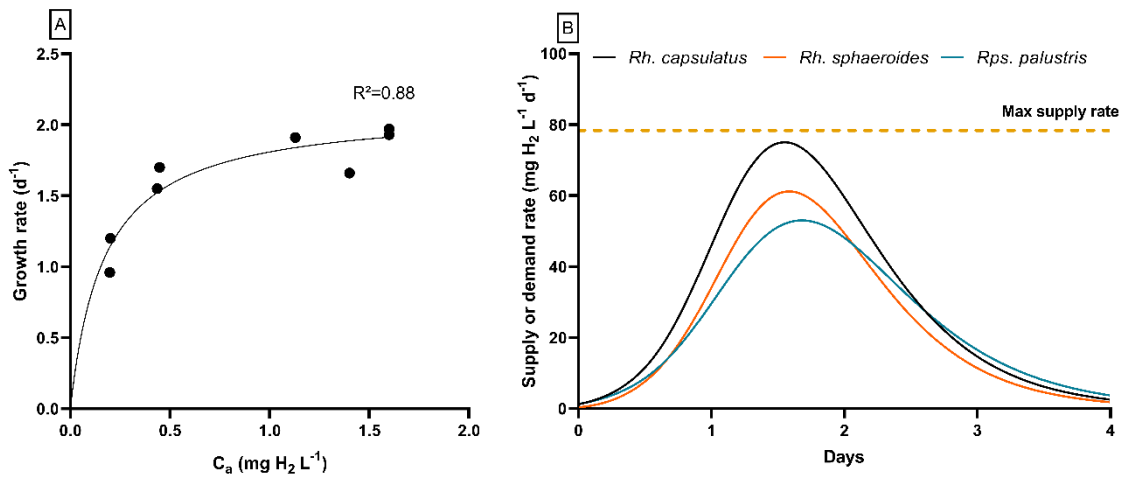
757

758 Figure 2: Comparison between maximum overall protein productivities (often achieved at stationary phase) of
 759 microbial protein sources (Ishizaki and Tanaka 1990, Ogbonda *et al.* 2007, Hempel *et al.* 2012, Matassa *et al.* 2016,
 760 Sui and Vlaeminck 2018, Alloul *et al.* 2019, Capson-Tojo *et al.* 2020) that express metabolic similarities with
 761 photohydrogenotrophic purple bacteria. The maximum protein productivities of photohydrogenotrophic purple
 762 bacteria are based on this study. To improve the visibility of the different box plots, the y-axis was divided in 3
 763 segments with varying ranges. For each boxplot, the number of observations is given.



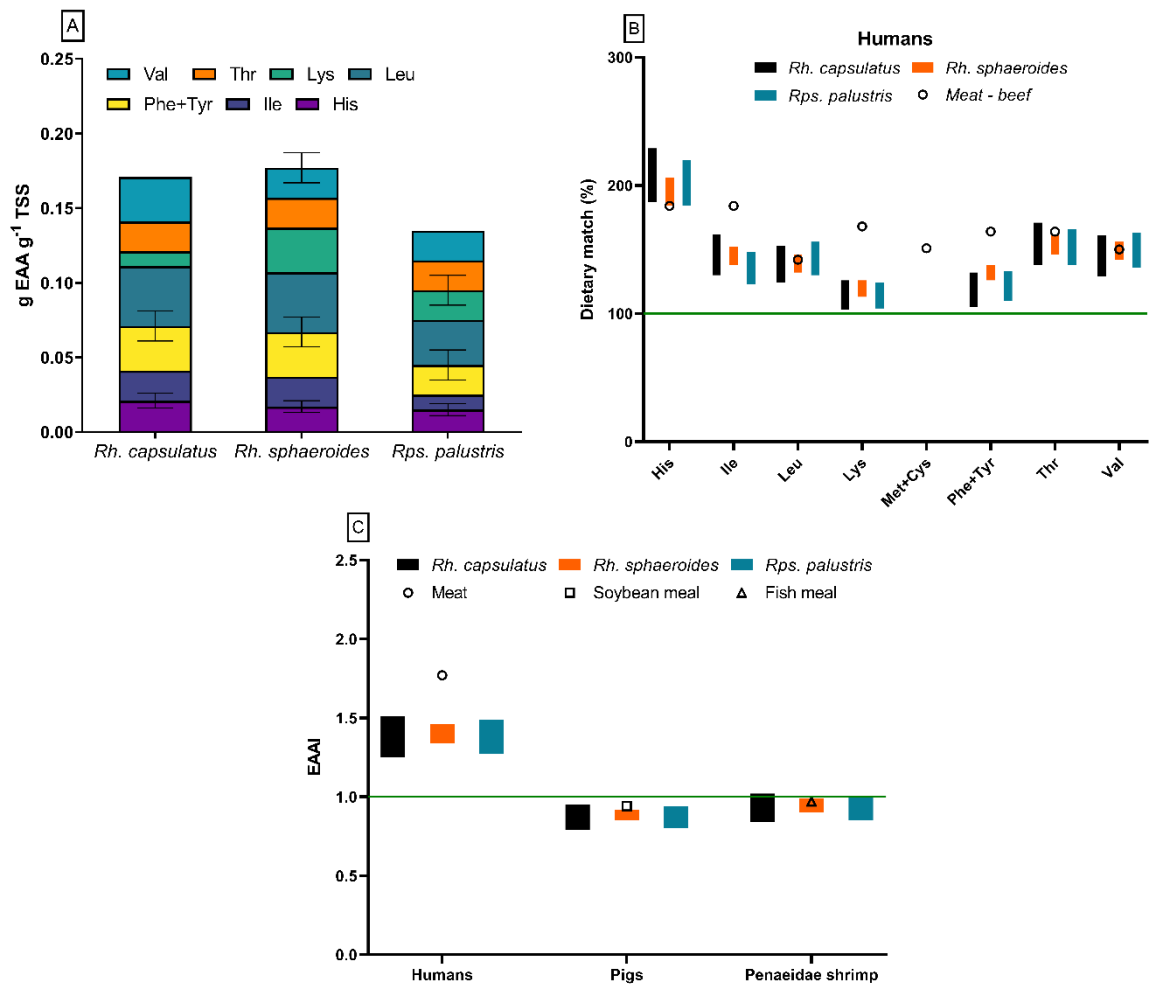
764

765 Figure 3: H₂-based yields of biomass resp. protein production (panel A resp. B) for *Rhodobacter capsulatus*,
 766 *Rhodobacter sphaeroides* and *Rhodospseudomonas palustris* at the stationary phase (t=4 days). Average values with
 767 standard deviations are given (n=3). Letters denote significant differences (p<0.05). Minimal and maximal empirical
 768 yields of hydrogen oxidizing bacteria are given as dashed yellow lines (Ishizaki and Tanaka 1990, Matassa *et al.*
 769 2016)
 770



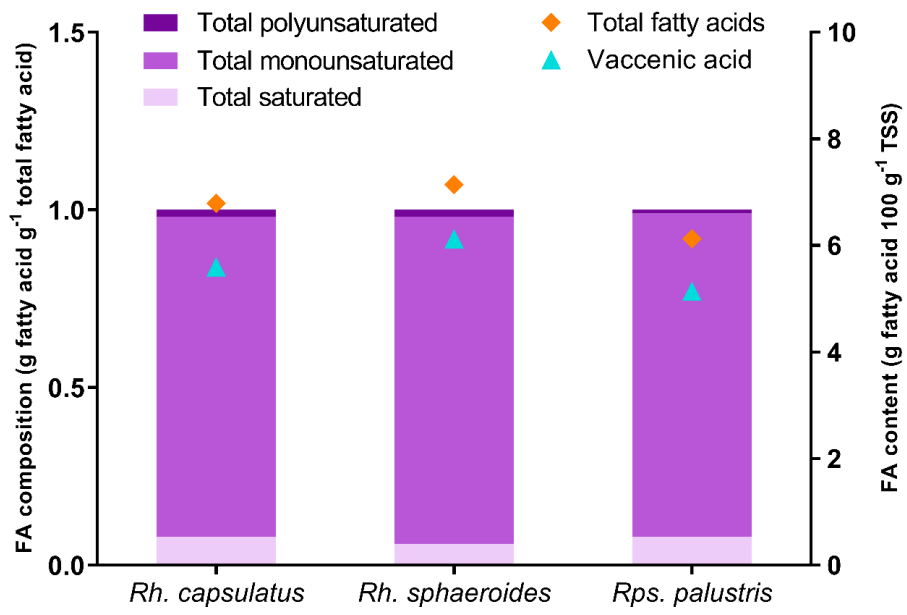
771

772 Figure 4: Hydrogen gas Monod model (panel A) based on the data points found in batch experiments with
 773 *Rhodobacter capsulatus* (n=8) at various estimated dissolved H₂ concentrations. Demand rates of hydrogen gas over
 774 the course of the batch experiment (panel B) for the three purple bacteria species (full lines) and the maximum
 775 supply rate (dashed yellow line).



776

777 Figure 5: Essential amino acid (EAA) profile and total EAA content expressed per g of total suspended solids (TSS) for
 778 three photohydrogenotrophically grown purple bacteria (*panel A*); Dietary match between the EAA in the purple
 779 bacteria and meat (beef) for humans (*panel B*); and the essential amino acid index (EAAI) for humans, pigs and
 780 Penaeidae shrimp (*panel C*). Standard deviations are given ($n=2$), but are omitted from *panel B* and *C* to increase
 781 visibility of the data.



782

783
784

Figure 6: Fatty acid (FA) composition and content in *Rhodobacter capsulatus*, *Rhodobacter sphaeroides* and *Rhodospseudomonas palustris* at the stationary phase (n=1).